Development of Testing Conditions for Gas/Surface Interaction Studies in Atmospheric Reentry Simulations

José Pedro Pinto Leite[1,2]

[1]*Instituto Superior Técnico, Technical University of Lisbon, Portugal*
[2]*von Kármán Institute for Fluid Dynamics, Belgium*

Abstract

Since the beginning of the space exploration that the design of the thermal protection system ("heat shield") of a planetary reentry vehicle (a vehicle that enters the atmosphere of a planet coming from the outer space) had been a challenge for the design engineers. Problems arise because of lack of fully comprehension on the physico-chemical processes involved, specifically Aerothermodynamics and Gas/Surface Interactions. In this thesis, the Local Heat Transfer Simulation methodology is used to fully reproduce the aerothermochemical conditions on the nose stagnation point of a reentry vehicle in a ICP Plasma Windtunnel, the Plasmatron, installed at the von Kármán Institute and capable of produce high enthalpy flows.

A pioneer testing methodology was developed to be used in high enthalpy facilities in order to understand the effect of surface temperature in surface recombination coefficient (catalycity) and heat flux from the plasma to the wall. Preliminary data was obtained and a sensitivity analysis was performed to access the reliability of the method. Plus, is proposed a method to construct a computationally efficient AeroThermodynamic DataBase (ATDB) for emissivity, catalycity and heat flux to be used in design and CFD codes and applicable both for passive and active concepts of thermal protective systems.

Keywords: *Thermal Protective Systems, Ground Testing, Gas/Surface Interactions, Aerothermodynamics, Catalycity*

Symbols

H	Specific Total Enthalpy	J kg^{-1}
h	Specific Enthalpy	J kg^{-1}
$\vec{J}$	Mass Flux	kg m^{-2} s^{-1}
$\vec{n}$	Normal to the Wall	-
PW	Power	J s^{-1}
p	Pressure	Pa = kg m^{-1} s^{-2}
q	Heat Flux	W m^{-2}
T	Temperature	K
β	Velocity Gradient	s^{-1}
γ	Catalycity	-
ε	Emissivity	-
λ	Thermal Conductivity	W kg^{-1} K^{-1}
ρ	Density	kg m^{-3}
σ	Stefan-Boltzmann constant	5.670373×10^{-8} W m^{-2} K^{-4}

Superscripts

F	relative to flight
GT	relative to the ground test
$\wr$	transferred to the surface
$\wr$	leaving the surface

Subscripts

$cond$	conductive
cw	cold wall
d	dynamic
$diff$	diffusive
e	boundary layer outer edge
el	electric - imposed on the HFreq generator
exp	experimental
i	relative to specie i
s	static
t	total
w	wall

I. Introduction

During reentry, a spacecraft travels in a speed much higher than the speed of sound, the so called hypersonic speed (Mach>5). Because of it, a strong bow shock wave is formed in the front of the vehicle. In the nose stagnation point region, the shock wave is almost a normal shock wave and through it the flow is decelerated to subsonic speeds and both pressure and temperature increase by several orders of magnitude. In a reentry from earth's orbit the temperature is usually high enough to promote dissociation in the gas and for a spacecraft returning from the moon or Mars it's usually enough to promote ionization [1].

Thermal protection systems can be divided in 3 main groups: Active, Passive and Semi-Passive. Figure 1 represents most of the current concepts for TPS and detailed information about each one can be found in [2, 3]. Until now, it was only possible to test Hot Structure, Insulated Structure and Ablation types in the von Kármán Institute (VKI).

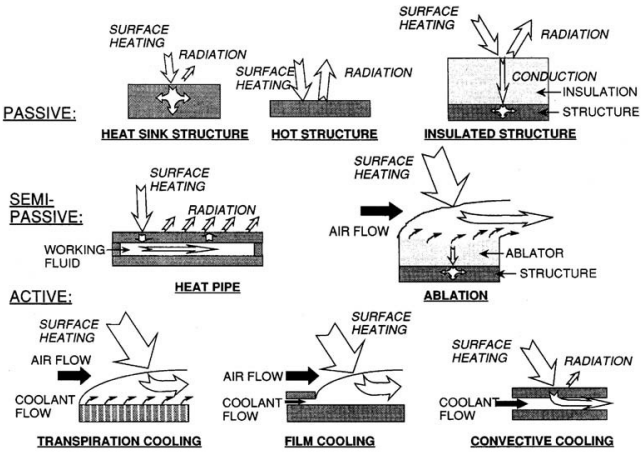

Figure 1: Thermal Protection System Concepts (extracted from [2])

II. The Local Heat Transfer Simulation methodology

In order to correctly duplicate the reentry flight conditions in a ground test facility it's mandatory to use similitude relations. It is known that practical ground test facilities can't totally reproduce the freestream of flight conditions with Mach numbers higher than 8 [4].

To overcome this problem Kolesnikov, at the *Institute for Problems in Mechanics* in Moscow, developed the LHTS methodology based on ICP plasma generators. This method allows to know with accuracy the stagnation point boundary layer edge conditions of a body immersed into a plasma jet and those condition can then be used to extrapolate the ground test to a real hypersonic flight condition [4, 5].

The base for the LHTS method are the analytical formulas developed in the 50s by Lees [6], Fay & Riddell [7] and Goulard [8].

Analysing these formulas, Kolesnikov [5] concluded that to simulate the reentry aerothermochemical environment at the stagnation point, only three parameters at the boundary layer edge need to be equal to the flight condition: total enthalpy, total pressure and velocity gradient [5, 4, 9].

$$H_e^F = H_e^{GT} \qquad p_{t,e}^F = p_{t,e}^{GT} \qquad \beta_e^F = \beta_e^{GT} \tag{1}$$

Conceptually, these 3 parameters represent the conditions behind the bow shock wave that appears in the front of an hypersonic vehicle (see figure 2).

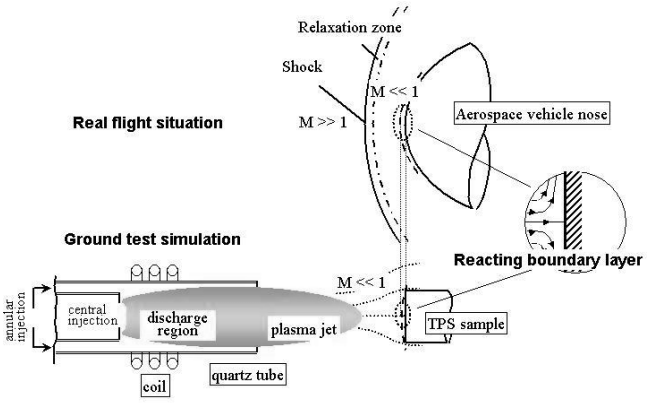

Figure 2: Ground Testing in a Plasmatron Facility under LHTS conditions

III. Plasmatron: The VKI's ICP Windtunnel

To produce plasma, this facility uses a physical principle called inductive-coupled plasma generation (ICP).

Conceptually it consists in a quartz tube surrounded by a coil in which a gas is injected. The coil is connected to a high power generator that provides high alternate voltage with an high frequency. The current in the coil induces a powerful oscillatory electro-magnetic field inside the tube with the field lines coaxial it. The residual charged particles in the gas are than accelerated because of the magnetic field and additional Foucault currents appear.

This makes the gas to heat up because of Joule's effect promoting an increase on the gas ionisation degree, increasing the Foucault currents and making the flow entering into an heating "snowball" effect that results in high temperature, highly ionized gas (plasma) that exits the torch in form of a jet.

The high power generator is capable of providing 1.2MW at 2kV and 400kHz and it's a solid state MOS technology generator. The torch as 160mm of diameter and exits to a test chamber at low pressure with 2.5m long and 1.4m diameter and the whole facility is cooled by deionized water in a close circuit. The facility is computer controlled using a 719 I/O lines PLC and two PC's for monitoring the operation [10, 11].

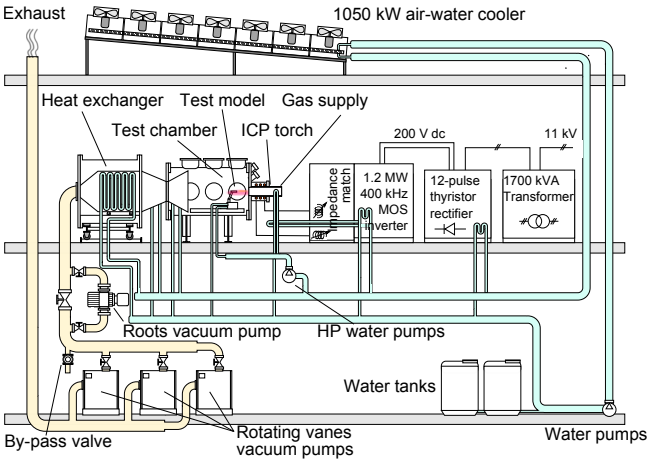

Figure 3: Plasmatron Facility

IV. Experimental Methods for Reentry Simulation in Plasmatrons

To extrapolate the test of a TPM sample exposed to plasma to a flight condition a multi-step methodology is used.

First, after the test and knowing the Plasmatron operation conditions (mass flow rate, chamber static pressure and electric power imposed on the high frequency generator) is possible to calculate the corresponding Non-Dimensional Parameters at the boundary layer edge using the ICP code, a viscous reactive flow solver coupled with an electro-magnetic solver [12, 13, 14].

During the test, a water cooled copper calorimeter is injected into the jet and the heat flux and surface temperature are recorded, being the surface catalycity estimated by the *Minimax* method in a different experiment [11, 15, 16].

With all these results, we can than use the the CERBOULA code[1] in order to calculate the boundary layer edge enthalpy (H_e) and other relevant properties in the boundary layer and on its edge.

At this point, we can extrapolate the results to flight conditions using boundary layer edge conditions and the equations presented in [4].

If one is also interested in the TPM catalycity, the process can than be reversed: The boundary layer edge parameters are now known, plus the surface temperature and heat flux (by optical methods [10] so the CERBOULA code can be run in order to determine the surface catalycity. Also the Kolesnikov's abacus [4] can be calculated and used for the same propose.

An important remark should be done about the way how the transferred heat flux is calculated. It is done by performing an energy balance at the surface of the sample:

$$q_w^{\downarrow} = q_w^{\uparrow} \tag{2}$$

$$q_{cond} + q_{diff} = q_{rad,out} + q_{loss} \tag{3}$$

$$\left(-\lambda\frac{\partial T}{\partial y}\right)_{\text{w,flow}} + \sum^{species} h_i \vec{J}_i \bullet \vec{n}_w = \sigma\varepsilon T_w^4 + \left(-\lambda\frac{\partial T}{\partial y}\right)_{\text{w,solid}} \tag{4}$$

V. Sample Holders

The sample holder consists in the support to expose the sample into the flow and stabilizing the velocity gradient. In this campaign, the holders had the shape presented in figure 4 with R_b=25mm and R_c=10mm.

[1] Also known as the VKI Boundary Layer code, thic code allows to reconstruct stagnation point aerothermochemical boundary layers [10].

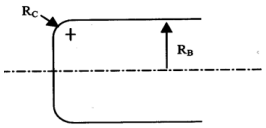

Figure 4: Holder Shape & Dimensions

In figure 5 is possible to see the classical sample holder used in VKI and the old location of the calorimeter that read the q_{loss} term (see section 4) in the classical setup. Previous experiments [15] showed that this quantity is negligible thanks to the thick layer of Procelit™ 180 placed in the back of the sample, so the calorimeter wasn't used in this setup for the tests presented in this work.

A new setup for the sample holder is presented in figure 6. It was developed with the purpose of lowering the temperature of the sample by heat conduction from the exposed surface of the sample to a calorimeter in its back that also measures q_{loss}, after proper treatment of the data [17].

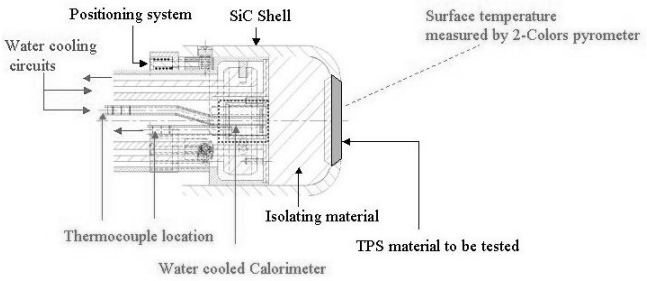

Figure 5: Classical Sample Holder - Radiative Equilibrium Setup

VI. Testing Procedures

Three tests were done and followed the testing sequence which is described below. In each test two samples were tested: one with the cooled setup and one with the classical insulated setup. From now on the sample installed in the cooled setup will be referred as cooled sample (CS) and the other as radiative equilibrium sample (RS). Each test correspond to a different pair of (p_e, β_e) because we tried to keep H_e constant.

In table 1 the test conditions are presented as well as some reference results extracted from the work of

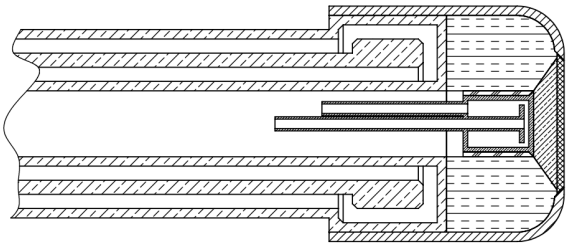

Figure 6: Sample Holder - Cooled Sample Setup

Panerai [11]. The target heat flux was calculated before the tests in order to match a BL edge enthalpy of 10MJ/kg.

Test Sequence:

- Chamber vacuum and pressure stabilization;
- Plasma generator and data recording start-up;
- Heat flux probe injection and power adjustment to the target heat flux;
- Heat flux probe retraction and cooled sample injection;
- Cooled sample exposure to plasma for approx. 8 minutes;
- Cooled sample retraction and radiative equilibrium sample injection;
- Radiative equilibrium sample exposure to plasma for approx. 8 minutes;
- Plasma off and chamber ventilation;
- Stop of data recording;
- Samples recovery after system cooling;

VII. Results

The results of the campaign are summarized in table 2.

In figure 7 we present the Kolesnikov's abacus for test T2 and one can observe some important heat flux quantities. The abacus for the other tests are similar.

The catalycity and heat flux results are plotted in a 3D graphic including all the boundary condition variables (except enthalpy that is considered constant) and the results are presented in figures 8 and 9 together

Test	Sample	q_{cw} kW m^{-2}	p_s Pa	p_d Pa	PW_{el} kW
T1-CS	S4	343	1440	93	138
T1-RS	S1	343	1440	93	138
S6 [11]	-	360	1300	83	99
T2-CS	S5	381	5000	31	149
T2-RS	S2	381	5000	31	149
S10 [11]	-	390	5000	27	130
T3-CS	S6	303	10000	13	142
T3-RS	S3	303	10000	13	142
C2a [11]	-	315	10000	11.8	137

Table 1: Test Conditions for the Temperature Campaign and Reference [11]

Test	β_e s^{-1}	T_w K	ϵ	q_{rad} kW m^{-2}	q_{loss} kW m^{-2}	q_{exp} kW m^{-2}	T_e K	p_e Pa	H_e MJ kg^{-1}	ρ_e kg m^{-3}	γ_{ref}	γ
T1-CS	6925.0	1375	0.82	167	43.7	210	4223	1440	9.3777	0.0009677418	0.10	0.026205
T1-RS	6925.0	1513	0.86	257	0.0	257	4223	1440	9.3777	0.0009677418	0.10	0.079643
S6 [11]	7277.0	1400	0.79	172	0.0	172	4440	1300	10.2487	0.0008190640	0.10	0.007280
T2-CS	2168.5	1374	0.78	157	52.8	210	4354	5000	9.4236	0.0032728925	0.10	0.005751
T2-RS	2168.5	1528	0.82	254	0.0	254	4354	5000	9.4236	0.0032728925	0.10	0.018183
S10 [11]	2097.8	1400	0.86	187	0.0	187	4485	5000	9.8197	0.0031588285	0.10	0.002204
T3-CS	935.2	1367	0.79	157	40.2	197	4085	10000	8.6575	0.0070697653	0.01	0.004082
T3-RS	935.2	1449	0.94	235	0.0	235	4085	10000	8.6575	0.0070698046	0.01	0.011544
C2a [11]	916.7	1515	0.90	269	0.0	269	4306	10000	9.1462	0.0066631346	0.01	0.023190

Table 2: Test Results From the Experiments and Reference [11]

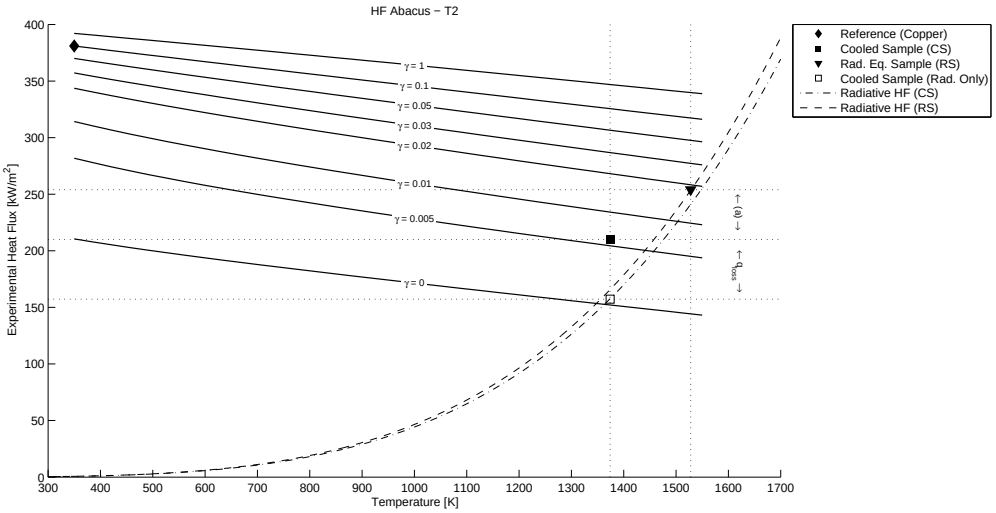

Figure 7: Abacus of test T2 - (a): Reduction on the experimental heat flux due to the reduction on the surface temperature

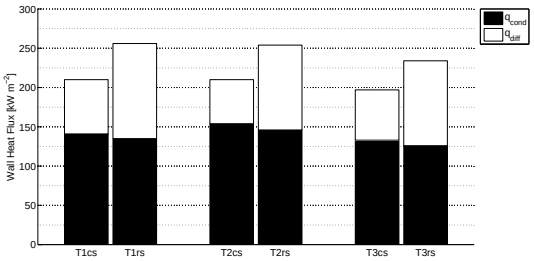

Figure 10: Heat Flux to the Wall

with the results from [11]. A 2D version of the graph can be also plotted to increase the readability but one should remember that p_e and β_e are independent parameters [18] and in order create the plot the β_e values were approximated (the approximation error is around 10%).

Appears that the slope of $\log(\gamma)$ vs. T_w doesn't evolve with (p_e,β_e), which means that γ is more sensible to T_w for (low p_e, high β_e) values. On the other hand, the slope of heat flux vs. T_w seams to be independent of (p_e,β_e).

In figure 10, one can see that cooling the sample (reducing T_w) conducts to an increase in the q_{cond} term but also to a major decrease in the q_{diff} term, due to catalycity decrease, which results in a global reduction of $q_w^{\searrow}$.

VIII. Sensitivity Analysis

A sensitivity analysis on the catalycity rebuilding process was done considering that errors on q_{loss} measurement and correction can occur. Experiment T1 was selected for the sensitivity study and the results are presented in table 3. One should note that even if the q_{loss} term had been underestimated by half of its value, the value of γ would still be lower than the value measured in the RS.

IX. Stagnation Point ATDB Algorithm

The ultimate target of TPS testing is to help the decision process and dimensioning of the TPS to be installed in future space missions.

Nowadays, very old and conservative formulas to estimate the heat transfer to the wall are still in use. This happens because design engineers like to have very simple formulas in order to introduce them in the fast optimization loops used during the preliminary-design phase of a project. The objective is always to know the heat flux from the plasma to the wall and it's known that it depends on 4 parameters: H_e,p_e,β_e,T_w besides surface material and gas mixture [4, 19, 17]. In fact, for a given material and gas mixture the heat flux dependencies can be summarized in the following formulas.

$$q_w^{\searrow} = q_w^{\nwarrow} \tag{5}$$

$$q_w^{\searrow} = f(H_e, p_e, \beta_e, T_w) \tag{6}$$

$$q_w^{\nwarrow} = f\left(T_w, \left(-\lambda \frac{\partial T}{\partial y}\right)_{\text{w,sol}}, \varepsilon(T_w)\right) \tag{7}$$

In equation 6 we could also include $\gamma \equiv f(T_w, ...)$ as a variable but it is a characteristic of the material.

Using the current setup in the Plasmatron, it is possible to make complete reconstruction of the stagnation point boundary layer of a body immersed in an hypersonic flow (valid for steady-state). Then, knowing the conditions at the boundary layer edge and at the wall, it is possible to obtain all the other relevant properties. One should remember that the cooled setup allows to select the surface temperature and also that catalycity depends on wall temperature.

With all this in mind, the correct way to construct a steady-state ATDB seems to be the one presented in the figures 11 and 12. For each flight condition, should be done a set of tests to access different velocity gradients (it varies with nose radius and flight conditions). For radiative equilibrium TPS types (Hot Structure and Insulated Structure) this is enough and the wall temperature is also a result but for semi-passive or active TPS types (see section 1), additional tests for several wall temperatures must be conducted.

All the information can then be stored in tables and allow a fast and easy method to know heat flux or catalycity to be implemented in future design or CFD codes.

In the figures, the thick boxes represent the inputs for the ATDB and the thick dashed boxes the results from the ATDB.

X. Conclusions

A new method for TPS testing was developed, allowing now the tests of Convective Cooling, Heat Pipe

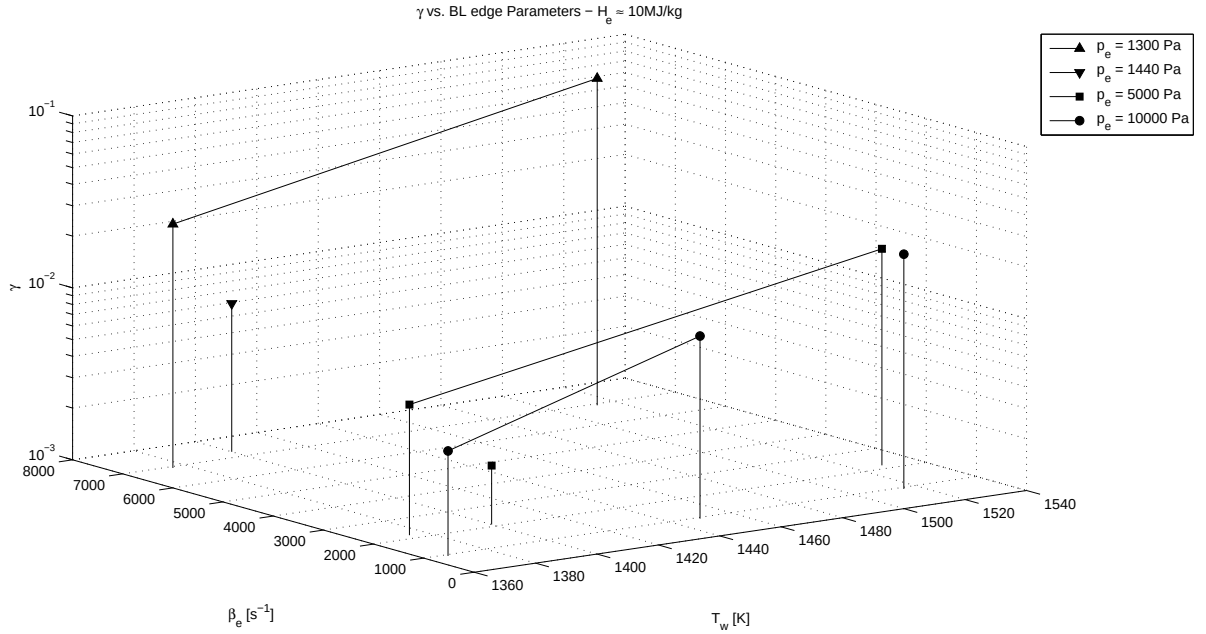

(a) Complete Plot

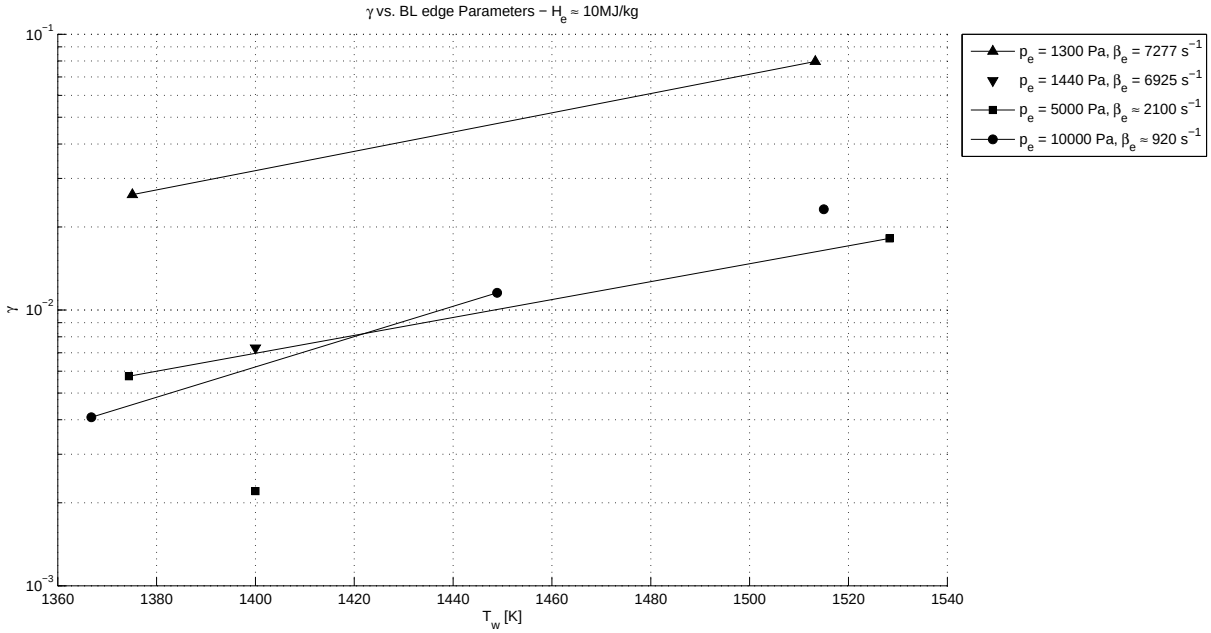

(b) Approximate Plot

Figure 8: γ as function of the BL edge parameters

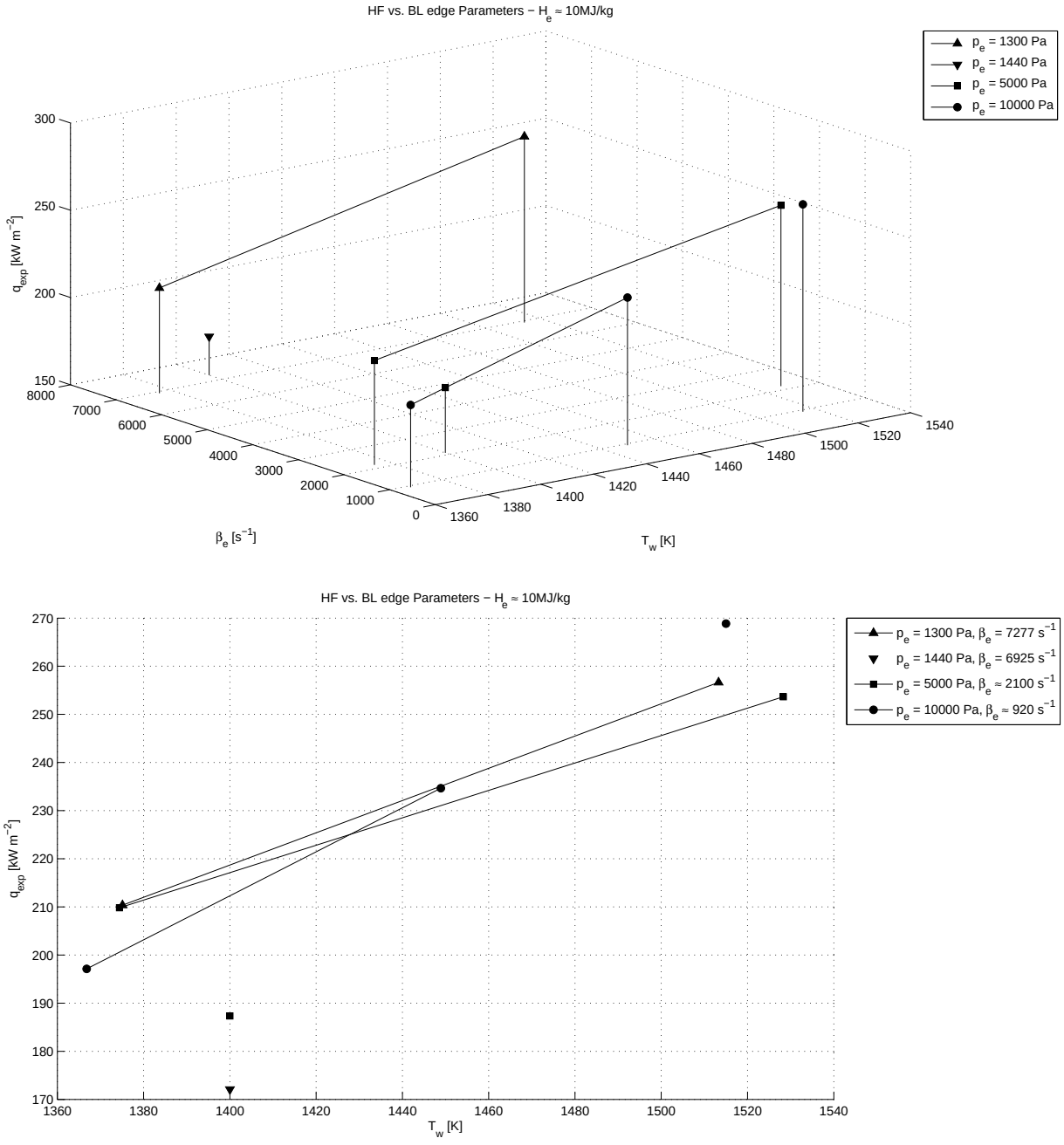

Figure 9: Experimental HF as function of the BL edge parameters

Variation in q_{loss}	q_{loss} [kW m^{-2}]	γ	γ Rel. Error [%]
-50%	21.9	0.01562	40.4
0%	43.7	0.02621	-
+10%	48.1	0.02877	9.8
+50%	65.6	0.04109	56.8
+100%	87.4	0.06349	142.3

Table 3: Sensitivity Analysis for Test T1

and Heat Sink Structure TPS in the VKI's Plasmatron. This new method also allows the correct study of the wall temperature effect on catalycity for fixed flight conditions. Experiments realized have shown that both catalycity and heat flux to the wall decrease by decreasing the surface temperature. It was also discovered that γ is more sensible to variations in T_w for (low p_e, high β_e) values and that the sensitivity of the heat flux to variations on T_w seems to independent of (p_e,β_e).

Efficient computational methods for construction and use of stagnation point aerothermodynamic databases were also presented.

XI. References

[1] Anderson, J. D. *Hypersonic and High Temperature Gas Dynamics*. AIAA, New York, 2nd edition, (2006).

[2] Kelly, H. N. and Blosser, M. L. In *Current Technology for Thermal Protection Systems, NASA CP 3157*, (1992).

[3] Glass, D. E. In *15th AIAA International Space Planes and Hypersonic Systems and Technologies Conference*, AIAA 2008-2682 (, Dayton, OH, USA, 2008).

[4] Kolesnikov, A. F. In *Educational Notes RTO-EN-AVT-008*. RTO, (1999).

[5] Kolesnikov, A. F. *Fluid Dynamics* **28**(1), 131–137 (1993).

[6] Lees, L. *Jet Propulsion* **26**(4), 259–269, 274 (1956).

[7] Fay, J. A. and Riddell, F. R. *Journal of Aeronautical Science* **25**(2), 73–85 (1958).

[8] Goulard, R. *Jet Propulsion* **28**(11), 737–745 (1958).

[9] Barbante, P. F. and Chazot, O. *Journal of Thermophysics and Heat Transfer* **20**(3), 493–499 (2006).

[10] Panerai, F. and Chazot, O. *Materials Chemistry and Physics* **134**(2-3), 597 – 607 (2012).

[11] Panerai, F. *Aerothermochemistry Caracterization of Thermal protection Systems*. PhD thesis, Università degli Studi di Perugia, von Kármán Institute for Fluid Dynamics, February (2012).

[12] Vanden Abeele, D., Bottin, B., Degrez, G., and Sarma, G. S. R. *Journal of System Anlysis, Modeling and Simulation (SAMS)* **34**(2), 169–187 (1999).

[13] Degrez, G., Barbante, P., de la Llave, M., Magin, T., and Chazot, O. In *European Congress on Computational Methods in Applied Sciences and Engineering, ECCOMAS Computational Fluid Dynamics Conference* (, Swansea, Wales, UK, 2001).

[14] Degrez, G., Vanden Abeele, D. P., Barbante, P. F., and Bottin, B. *International Journal of Numerical Methods for Heat & Fluid Flow* **14**(4), 538–558 (2004).

[15] Chazot, O. In *Course on Hypersonic Entry and Cruise Vehicles*. Stanford University and NASA Ames Research Center (in collaboration with von Karman Institute for Fluid Dynamics), (2008).

[16] Krassilchikoff, H. W., Chazot, O., and Thoemel, J. In *2nd European Conference for Aero-Space Sciences (EUCASS)* (, Bruxelles, Belgium, 2007).

[17] Pinto Leite, J. P. S. STP 2012-18, von Kármán Institute for Fluid Dynamics, (2012).

[18] Chazot, O., Panerai, F., and Marotta, M. In *7th European Aerothermodynamics Symposium* (, Brugge, Belgium, 2011).

[19] Chazot, O., Panerai, F., and Van Der Haegen, V. In *17th AIAA International Space Planes and Hypersonic Systems and Technologies Conference*, AIAA 2011-2210 (, San Francisco, CA, USA, 2011).

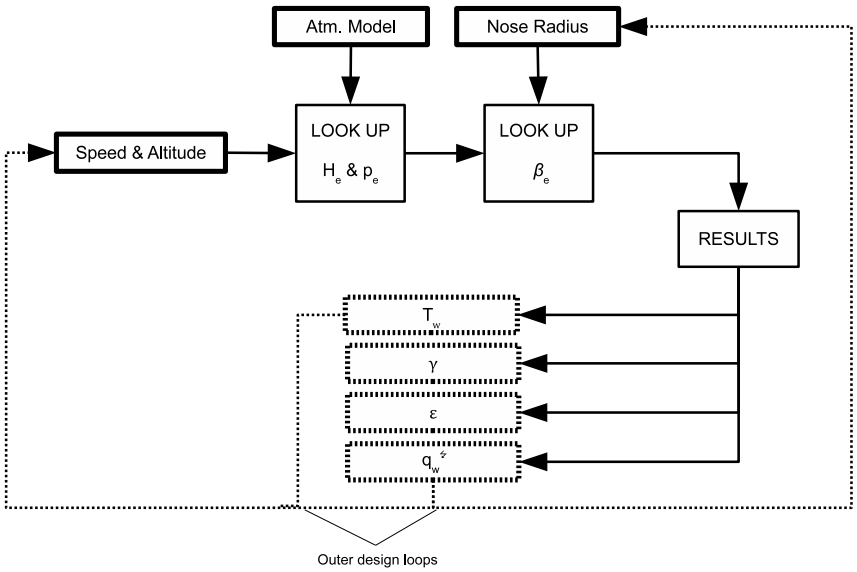

Figure 11: Flowchart for ATDB Algorithms - Hot or Insulated Structure TPS

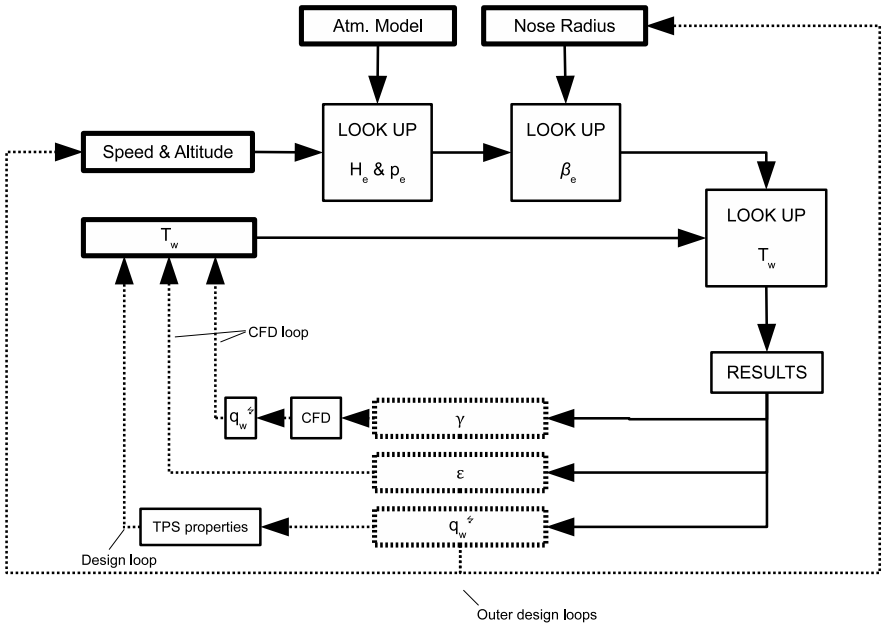

Figure 12: Flowchart for ATDB and Algorithms - Generic TPS